SOVIET PHYSICS

JETP

A translation of the Journal of Experimental and Theoretical Physics of the USSR.

SOVIET PHYSICS—JETP VOL. 5, NO. 1, PP 1-155 AUGUST, 1957

Investigation of the (γ, p) Reaction in Zinc

R. M. OSOKINA AND B. S. RATNER

The P. N. Lebedev Physical Institute of the Academy of Sciences USSR

(Submitted to JETP editor June 1, 1956)

J. Exptl. Theoret. Phys. (U.S.S.R.) **32**, 20-26 (January, 1957)

Measurements of the yield and angular and energy distribution of photoprotons emitted from zinc have been carried out at various bremsstrahlung peak energies ranging from 19.8 to 30.7 mev. The results are compared with the statistical theory of nuclear reactions and with the direct photoeffect model. The data obtained with zinc confirm the conclusions regarding the significance of a direct photoeffect and of the influence of shells for nuclei with $Z \sim 30$.

1. INTRODUCTION

THE present work continues the investigation of photoprotons emitted by different nuclei under the action of synchrotron bremsstrahlung with γ-ray energies up to 30 mev[1-3].

As is well known, deviations from the statistical theory in the investigation of photonuclear reactions have been observed in a number of papers (Refs. 4-6 and others). In the investigation of the (γ,p) reaction in copper[1] and in nickel[2] a number of additional facts were discovered which contradict the idea of evaporation of particles from the compound nucleus. These results were qualitatively explained by assuming a direct interaction of the γ-quanta with the individual nucleons in the nucleus (the so-called "direct" photoeffect) with the shell structure of the nucleus taken into account.

In accordance with the shell model[7], the zinc nucleus has a structure analogous to the copper nucleus, with the only difference that outside the filled $4f_{7/2}$ level containing 8 protons, the zinc nucleus in the $3P_{3/2}$ state contains not one but two protons. Therefore, it was expected that investigations carried out with zinc would confirm the sharp change in the proton distribution accompanying a small increase in $E_{\gamma m}$ obtained in the case of copper and explained by assuming that the photoeffect from the $4f_{7/2}$ level begins to be important.

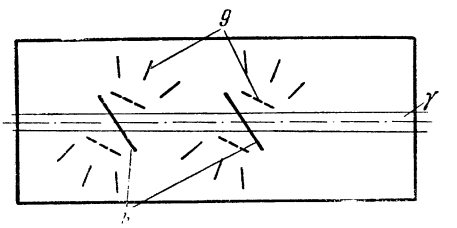

FIG. 1. Positioning of the plates. g — photo plates, h — targets, dotted lines indicate the position of the plates for the measurement of proton yield.

2. THE METHOD OF MEASUREMENT

The experimental method has been described in detail in Ref. 1. The protons were recorded in thick nuclear emulsions NIKFI Ia-2 400μ in thickness. The placing of the plates is shown in Fig. 1. The construction of the chamber in which the plates were situated was altered slightly in order to improve the positioning of the plates and the placement of the chamber with respect to the γ-ray beam. In order to remove soft electrons from

the beam permanent magnets were installed inside the chamber. The proton background was measured with the target removed from the chamber. It was of significant amount (5-10%) in only two plates which were nearest to the γ-beam. In the other plates the proton background did not exceed 1%. The background is primarily due to protons with energies up to 5-6 mev. The target was in the form of a foil of chemically pure zinc of 25 mg/cm^2 in thickness. The energy losses in the half thickness of the target were calculated in accordance with Ref. 8. The emulsions were treated by the dry temperature method using the standard amidol developer. The plates were scanned by means of binocular microscopes MBI-2 with a magnification of 630X. In scanning the plates proton tracks were selected corresponding to proton energies $\epsilon_p \geq 3.0$ mev which started at the surface of the emulsion and proceeded in the required direction. The complete energy spectrum was measured in only two irradiations at energies $E_{\gamma m} = 20.8$ and 28.6 mev. In all the other cases only the energy of the fast protons with $\epsilon_p \geq 9$ mev was determined. The proton energy was determined from the range-energy curve for the Ilford C-2 emulsion[9], which is permissible because of the similarity in the composition of the emulsions NIKFI Ia-2 and Ilford C-2. No identification of deuteron tracks was made.

The dosage was recorded by means of an integrating ionization monitoring chamber. The monitor was calibrated by means of a thickwalled ionization chamber whose sensitivity was calculated according to the data of Ref. 10. The photon spectrum was found in accordance with Ref. 11 taking into account absorption in the walls of the accelerating chamber.

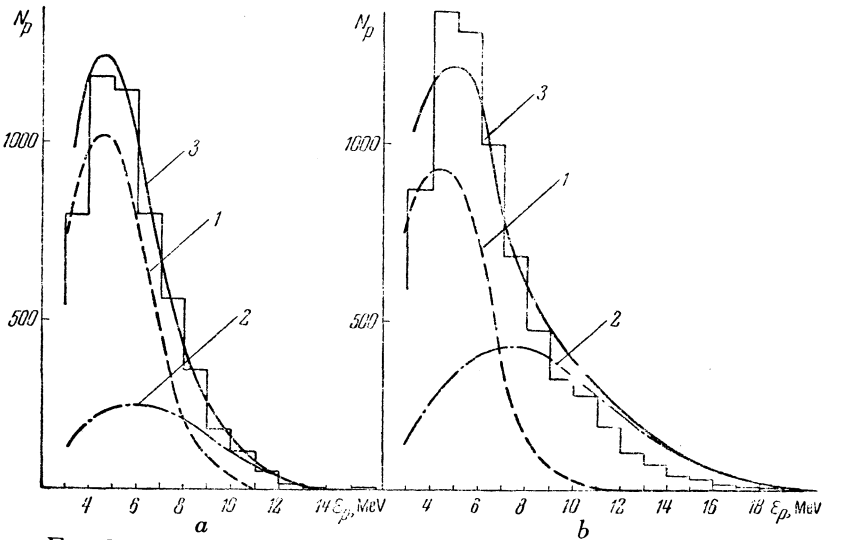

FIG. 2. Energy distributions of photoprotons from zinc obtained at energies $E_{\gamma m}$: *a* – 20.8 mev and *b* – 28.6 mev. *1* – spectra calculated according to evaporation theory; *2* – spectra calculated according to the direct photoeffect model[14] taking shells into account; *3* – the sum of curves 1 and 2.

3. EXPERIMENTAL RESULTS

Figure 2 shows the energy spectra integrated over the angles θ of the photoprotons with energies $\epsilon_p \geq 3$ mev from zinc, obtained at energies $E_{\gamma m} = 20.8$ and 28.6 mev. Curve 1 for $E_{\gamma m} = 20.8$ mev is normalized in accordance with the data on angular distribution on the assumption that its isotropic part (75%) is due to evaporation. For $E_{\gamma m} = 28.6$ mev, the normalization was carried out on the basis of the calculated dependence on $E_{\gamma m}$ of the yield of evaporated protons. The areas under curve 3 and under the experimental histogram are equal. The calculated curves include a correction for finite target thickness. Figure 3 shows energy distributions of photoprotons with energies $\epsilon_p \geq 9$ mev measured for various values of $E_{\gamma m}$. Figure 4 shows the angular distributions of photoprotons with energies $\epsilon_p \geq 3$ and $\epsilon_p \geq 9$ mev. The dependence of the yield

of protons with $\epsilon_p \geq 3$ mev on the maximum γ-ray energy $E_{\gamma m}$ is shown in Fig. 5. The proton yield is normalized to the same ionization in a thick-walled ionization chamber. Figure 6a shows the analogous dependence for photoprotons with $\epsilon_p \geq 9$ mev. obtained by multiplying the yield of protons with $\epsilon_p \geq 3$ mev (Fig. 5) by the ratio of the number of protons with $\epsilon_p \geq 9$ mev to the number of protons with $\epsilon_p \geq 3$ mev, taking the angular distribution into account. The errors shown in the Figures are statistical. Figure 6b shows the cross-section

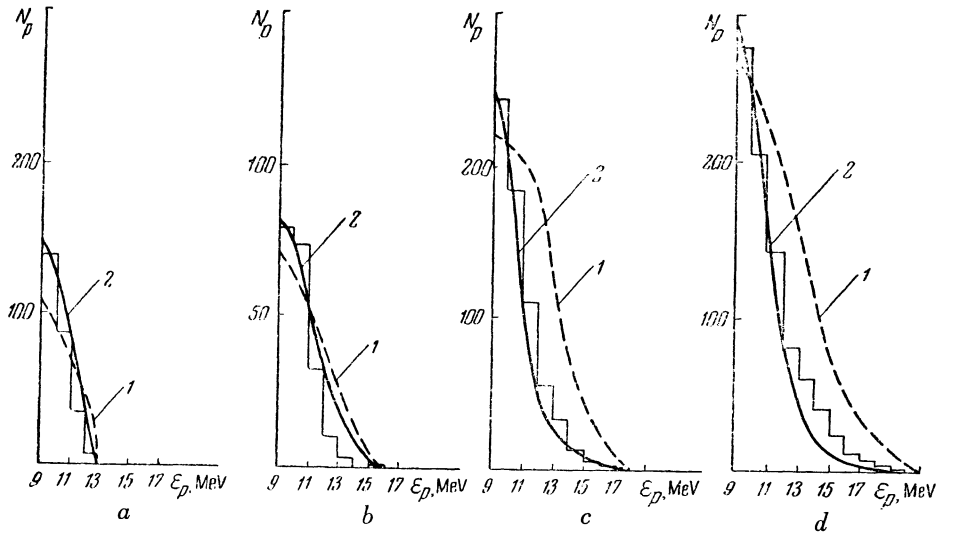

FIG. 3. Energy distributions for protons with energies $\epsilon_p \geq 9$ mev from zinc obtained at E_{γ_m} : a – 20.8; b – 23.3; c – 26.1 and d – 28.6 mev. The spectra have been calculated using the direct photoeffect model taking shells into account and utilizing: *1* – the cross sections from Ref. 14, *2* – the experimental cross-section.

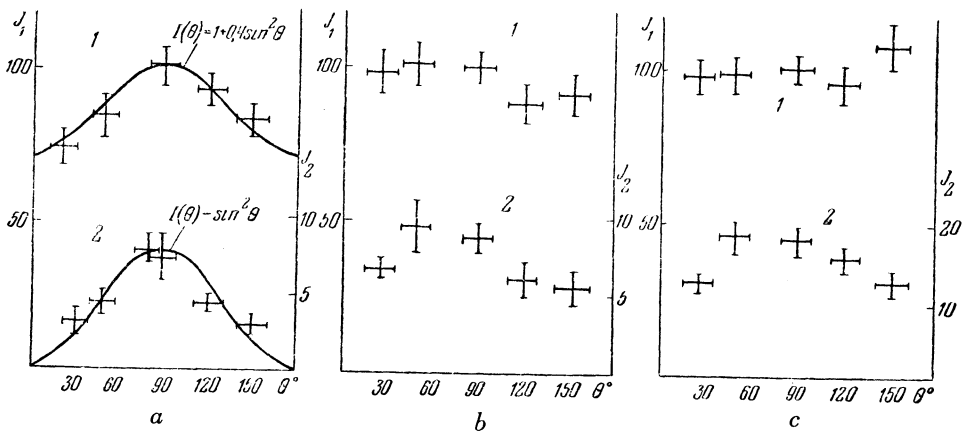

FIG. 4. Angular distributions of photoprotons from zinc obtained at energy values $E_{\gamma m}$: a – 20.8, b – 23.3 and c – 28.6 mev. I_1 and I_2 are the relative numbers of protons per unit solid angle for protons: *1* – with energies $\epsilon_p \geq 3$ mev, *2* – with energies $\epsilon_p \geq 9$ mev.

for the production of photoprotons with $\epsilon_p \geq 9$ mev calculated from the yield curves by the "photon difference" method[12]. An estimate of the integrated cross-section for the emission of photoprotons with energy $\epsilon_p \geq 3$ mev from zinc gives a value equal to 0.46 mev · barn. The ratios for the photoproton yield from zinc, copper and nickel at $E_{\gamma m} = 25.5$ mev are 1.5: 1.0: 1.7, respectively.

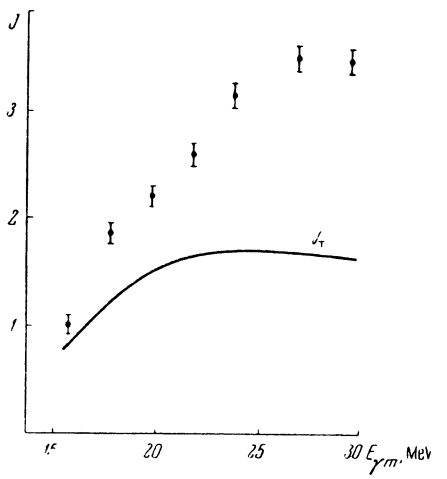

FIG. 5. Dependence on E_{γ_m} of the yield of photoprotons with energies $\epsilon_p \geq 3$ mev from zinc. I_T is the curve calculated according to evaporation theory and normalized according to the data on angular distribution on the assumption that at $E_{\gamma m} = 20.8$ mev the isotropic part of the yield (75%) is determined by evaporation. I is the yield in relative units reduced to the same ionization in a thick-walled ionization chamber.

4. DISCUSSION OF RESULTS

In the discussion of results, the most attention was devoted to the data obtained for fast protons since the direct photoeffect of interest to us should be particularly prominent in this energy region.

An examination of the angular distributions of photoprotons from zinc (Fig. 4) shows that a marked anisotropy for protons with energies $\epsilon_p \geq 3$ mev of the form $I(\theta) \sim 1 + 0.4 \sin^2 \theta$ for $E_{\gamma m} \leq 20.8$ mev* is replaced by a practically isotropic distribution for $E_{\gamma m} \geq 23.3$ mev. For fast protons with $\epsilon_p \geq 9$ mev the angular distribution for $E_{\gamma m} \leq 20.8$ mev has the form $I(\theta) \sim \sin^2 \theta$. For energies $E_{\gamma m} \geq 23.3$ mev an appreciable isotropic component appears and the maximum in the angular distribution is displaced forward.

Thus in zinc a sharp change in the angular distribution is observed as we go from $E_{\gamma m} = 20.8$ mev to $E_{\gamma m} = 23.3$ mev. Apparently this result, as in the case of copper, can be explained by assuming that at large γ-ray energies the photoeffect from the deeper lying level $4f_{7/2}$ begins to play a more important role. In this connection, it should be pointed out that the angular distributions obtained for fast photoprotons from zinc at $E_{\gamma m} \geq 23.3$ mev are somewhat similar to the angular distributions obtained in nickel[2] and in cobalt[13], i.e., in nuclei where the filling of the $4f_{7/2}$ shell is completed. These distributions also do not contradict the data obtained in the case of copper[1]. The displacement in the forward direction with respect to $\theta = 90°$ of the maximum of the angular distribution in all these cases apparently points to the fact that, for this level, interference between the dipole and the quadrupole absorption of γ-quanta takes place.

It should be noted that in the case of zinc the anisotropy in the angular distributions of fast protons for relatively small values of $E_{\gamma m}$ is too great, just as in the case of copper, in comparison with what is predicted in Refs. 14 and 15 for the photoeffect from the P-shell.

The angular distribution of the form $I(\theta) \sim \sin^2 \theta$ obtained for fast photoprotons from copper and zinc would appear to indicate a considerable transparency of these nuclei for protons from the uppermost level. In this case, however, the following consideration should be taken into account. The transfer by the proton of a considerable amount of energy on collision which could lead to a significant distortion of the angular distribution removes the proton from among the recorded fast protons.

The energy distributions of photoprotons from zinc obtained at $E_{\gamma m} = 20.8$ and 28.6 mev (see Fig. 2) were compared with spectra calculated on the basis of the statistical theory of nuclear reactions[16], and in accordance with the direct photoeffect model proposed in Ref. 14. In making the calculations using the statistical theory it was assumed that the level density of the final nucleus depends on its excitation energy E_R in

* The angular distributions obtained for $E_{\gamma m} = 19.8$ mev which are not shown in Fig. 4 are even more anisotropic than those for $E_{\gamma m} = 20.8$ mev.

accordance with[17] $\omega(E_R) = \text{const} \cdot \exp\{(3.35 \times (A-40)^{1/3} E_R)^{1/2}\}$; $E_R = E_\gamma - \epsilon_p - B_p$ where B_p is the proton binding energy. The calculation was made for the main isotope Zn^{64}. The ratio of the binding energies of the proton and the neutron in the other isotopes is such that their contribution to the total evaporation spectrum is quite small. The binding energies for the proton B_p and for the neutron B_n in Zn^{64} were taken to be 7.7 and 11.8 mev respectively[18].

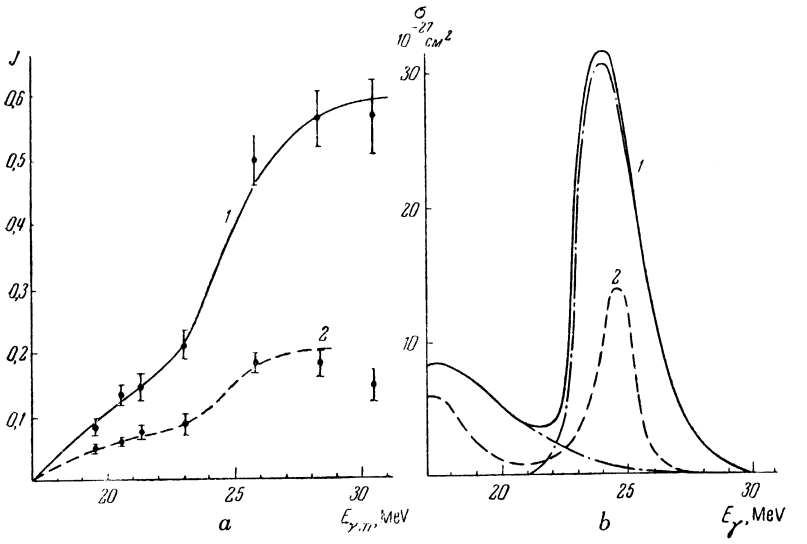

FIG. 6. a – dependence on $E_{\gamma m}$ of the yield of fast photoprotons from zinc; b – cross-section for the emission of fast protons from zinc. $1 - \epsilon_p \geq 9$, $2 - -8 \leq \epsilon_p \leq 10$ mev.

The calculation of the energy spectrum using the direct interaction model was carried out on the assumption that the protons in the nucleus are in separate levels with binding energies B_{p1}, B_{p2} etc., and that the total energy of the γ-quantum minus the binding energy is given up to the emitted proton. Transitions $l \to l-1$ and $l \to l+1$ were taken into account. The photoproton spectrum for the given isotope was found using the formula

$$N(\varepsilon_p) = \text{const} \cdot \sum_i n_i \sigma(\varepsilon_p + B_{p_i}) N_\gamma(\varepsilon_p + B_p, E_{\gamma m}) \times [g_{l_i-1} T_{l_i-1}(\varepsilon_p) + g_{l_i+1} T_{l_i+1}(\varepsilon_p)].$$

Here n_i and l_i are respectively the number of protons in the i-th level and their angular momentum in accordance with the model of filling the levels given in Ref. 7; $T_{l_i \pm 1}(\varepsilon_p)$ – the penetrability through the barrier – was calculated using the formulas given in Ref. 16; $g_{l_i \pm 1} = |2(l_i \pm 1) + 1|$ is the statistical factor; $N_\gamma(\varepsilon_p + B_{p_i}, E_{\gamma m})$ is the number of γ-quanta of energy $E_\gamma = \varepsilon_p + B_{p_i}$ in the bremsstrahlung spectrum with maximum energy $E_{\gamma m}$; $\sigma(\varepsilon_p + B_{p_i})$ is the cross-section for the direct photoeffect per nucleon taken from Ref. 14. As may be seen from Fig. 2, for $E_{\gamma m} = 20.8$ mev the experimental spectrum is well described by the sum of the theoretical curves. However, at $E_{\gamma m} = 28.6$ mev, the observed proton distribution shows a deficiency of fast and an excess of slow protons. This deviation may be explained either by assuming that as the energy of the proton increases the probability of it transferring a part of its energy to the other nucleons in the nucleus increases also, or by assuming that the dependence of the cross-section for the direct photoeffect on the energy of the γ-quanta differs from the one given in Ref. 14*. In this connection it is of interest to examine the

* It is of interest to note that a calculation of the direct photoeffect for the nucleus Mo^{100} carried out by B. N. Kalinkin (private communication) showed that the total cross-section is made up of the sum of the resonance cross-sections for individual levels.

data on the cross-section for the emission of fast protons from zinc. As may be seen from Fig. 6b the cross-section for protons with $\epsilon_p \geq 9$ mev has a sharp peak in the region of γ-quanta with energy $E_p \sim 23$-24 mev and falls off towards $E_\gamma \sim 29$-30 mev. Apparently there is also a second maximum at an energy of 17-18 mev but it is less pronounced. The cross-section curve plotted for protons with energy in the range 9-10 mev indicates more clearly the presence of two peaks in the cross-section which are most probably determined by the absorption of γ-quanta by protons in the two outer shells of the zinc nucleus. From the value of the energy of the γ-quanta at which the second rise in the cross-section for the emission of protons with $\epsilon_p \geq 9$ mev is observed it is possible to determine the position of the $4f_{7/2}$ level. The depth of this level is ~ 14 mev from which the value of ~ 6 mev is obtained for the distance between the two upper levels.

In order to check the correctness of the form of the cross-section curve, obtained from the yield curve with considerable errors, this curve was used to calculate the energy distribution of the photoprotons on the assumption of the transfer of the total energy of the γ-quantum minus the binding energy to the proton. The assumed form for the cross-section for the direct photoeffect for each of the upper levels is shown in Fig. 6b. As may be seen from Fig. 3, the spectra of fast photoprotons from zinc calculated using the experimental cross-section agree satisfactorily with the experimental spectra, while Courant's cross-section predicts a much harder proton energy spectrum.

A model for the nuclear photoeffect proposed by Wilkinson[15] has been widely discussed in recent literature. In contrast to the model of collective dipole oscillations of protons with respect to neutrons in the nucleus (Refs. 19, 20 and others), Wilkinson's model explains the "giant" resonance observed in photonuclear reactions in terms of the resonance absorption of γ-quanta by individual nucleons situated within closed shells. In this model the nucleons outside closed shells should play no essential role. However, as indicated by the angular distributions and by the cross-sections for protons obtained in the present work, and also by the results for copper[1], one or two protons in the new unfilled shell play an important role particularly for relatively low values of the energy of the γ-quanta. If the direct photoeffect were determined primarily by the closed shell then one would not expect the experimentally observed sharp change in the form of the angular distributions as the energy of the γ-quanta is varied. Also one would expect that the photoeffect in nickel, copper and zinc should not show appreciable differences.

Thus the results of studying photoprotons from zinc confirm the conclusions reached earlier that the contribution of the direct photoeffect to the proton yield from nuclei with $Z \sim 30$ represents a considerable amount (20-40%) at γ-ray energies used. It seems probable that in the above case the γ-quanta interact with protons situated within individual nuclear shells. Apparently the cross-section for such an interaction has a resonance character.

Indications of the influence of the shells were obtained in the recently published work on the investigation of photoprotons from argon[21]. Unfortunately, the data available for other elements are insufficient to be analyzed in terms of the considerations given above.

The authors are very grateful to R. D. Polukarova and N. A. Ponomareva for their help in scanning the plates, and in analyzing the results, and also to the members of the group operating the synchrotron.

---

1 Leiken, Osokina and Ratner, Dokl. Akad. Nauk SSSR **102**, 245 (1955).
2 Leiken, Osokina and Ratner, Dokl. Akad. Nauk SSSR **102**, 493 (1955).
3 Leiken, Osokina and Ratner, Supp. Nuova Cim. **3**, 105 (1956).
4 O. Hirzel and H. Waffler, Helv. Phys. Acta. **20**, 373 (1947).
5 B. C. Diven and C. M. Almy, Phys. Rev. **80**, 407 (1950).
6 P. R. Byerly and W. E. Stephens, Phys. Rev. **83**, 54 (1951).
7 P. F. Klinkenberg, Rev. Mod. Phys. **24**, 63 (1952).
8 J. Lindhard and M. Scharff, Phys. Rev. **85**, 1058 (1953).
9 J. Rotblat, *Nature* **167**, 550 (1950).
10 Flowers, Lawson and Fossey, Proc. Phys. Soc. (London) **65B**, 286 (1952).
11 G. D. Adams, Phys. Rev. **74**, 1707 (1948).
12 L. Katz and A. G. W. Cameron, Canad. J. Phys. **29**, 518 (1951).
13 M. E. Toms and W. E. Stephens, Phys. Rev. **95**, 1209 (1954).
14 E. D. Courant, Phys. Rev. **82**, 703 (1951).
15 D. H. Wilkinson, Proc. of the 1954 Glasgow Conference on Nuclear Physics.
16 J. Blatt and V. Weisskopf, *Theoretical Nuclear Physics* (Russian translation) 1955.
17 V. Weisskopf, *Statistical Theory of Nuclear Reactions* (Russian translation) 1952.
18 V. A. Kravtsov, Uspekhi Fiz. Nauk **54**, 3 (1954).
19 A. B. Migdal, J. Exptl. Theoret. Phys. (U.S.S.R.) **15**, 81 (1945).

20 M. Goldhaber and E. Teller, Phys. Rev. **74**, 1046 (1948).
21 B. M. Spicer, Phys. Rev. **100**, 791 (1955).

Translated by G. M. Volkoff
3

SOVIET PHYSICS JETP VOLUME 5, NUMBER 1 AUGUST, 1957

Electron Emission from Dielectric Films Bombarded by Positive Hydrogen Ions

V. Z. SURKOV
Kharkov State University

(Submitted to JETP editor May 18, 1956)
J. Exptl. Theoret. Phys. (U.S.S.R) 32, 14–20 (January, 1957)

An investigation has been made of the electron emission which is produced by bombarding dielectric films with positive ions and which continues after termination of the ion bombardment. The electron emission was excited by hydrogen ions, oxygen ions, and lithium ions. The emission has been observed in films of CaF_2, B_2O_3, Al_2O_3, and in mica sheets. The effect of target temperature on emission was investigated. The potentials at the film surfaces have been measured.

WHEN thin dielectric films deposited on a metal substrate are bombarded by electrons or ions, under certain conditions there is observed an extended electron emission which continues after the bombardment is terminated. The origin of this emission seems to be associated with the positive charge at the surface of the dielectric. Malter [1], who discovered this effect, and other investigators bombarded the surface of a dielectric film with electrons to obtain the emission. Starodubtsev[2] obtained this emission by creating a positive charge at the surface of a B_2O_3 film bombarded by K^+ ions and B_2O^+ ions.

The present work was undertaken to obtain more information on the electron emission from dielectric films, deposited on a metal substrate, which is produced when the films are bombarded by positive ions.

DESCRIPTION OF THE APPARATUS AND METHOD OF MEASUREMENT

The experiments were carried out with the apparatus shown in Fig. 1. The target 6 in the operating chamber 8 is bombarded by positive ions selected by the mass-analyzer 2. The instrument frame is grounded. Ions which leave the mass-analyzer pass through two diaphragms 3 with an aperture diameter of 4 mm. To inhibit secondary-electron emission from diaphragm 3, a negative potential of 300 volts is applied to the cylindrical electrode 4 (inner diameter 12 mm, length 15 mm). The target holder 7, which is insulated from the frame and is in electrical contact with the target 6, can be rotated without breaking the vacuum. The micrometer screw 9 is insulated from the frame and is used to move the probe 10 back and forth without disturbing the vacuum. The probe 10 can touch the target 6, as desired, in which case electrical contact is established between the target and the micrometer screw. It is also possible, without disturbing the vacuum, to position a flat disc-collector (not shown in Fig. 1) between the target and collector 5; this disc-collector is insulated from the frame but is in contact with the collector. The ion current is measured by the galvanometer G in the collector–target circuit when the collector potential $V_c = 0$. The electron emission curve is measured with the same galvanometer G, in the collector–target or disc-collector-target circuit, but with a positive collector potential V_c varying from 0 to 3,000 volts applied to the collector. The dielectric film is deposited on the target by vacuum evaporation in the operating chamber 8 while a vacuum of approximately 10^{-6} mm Hg is maintained. By rotating the rod 7, the targets are set over the evaporator 1, located in the bottom part of the operating chamber 8, and B_2O_3 and CaF_2 are evaporated on to the molybdenum substrate. After the film is evaporated, the target is positioned opposite the collector and subjected to ion bombardment. Before deposition of the film,